Design, Synthesis, and Antiviral Activity of Entry Inhibitors That Target the CD4-Binding Site of HIV-1

Francesca Curreli,[†] Spreeha Choudhury,[†] Ilya Pyatkin,[‡] Victor P. Zagorodnikov,[‡] Anna Khulianova Bulay,[‡] Andrea Altieri,[‡] Young Do Kwon,[§] Peter D. Kwong,[§] and Asim K. Debnath*,[†]

[†]Lindsley F. Kimball Research Institute, New York Blood Center, 310 E. 67th Street, New York, New York 10065, United States
[‡]Asinex Ltd., 20 Geroev Panfilovtzev, Building 1, Moscow 125480, Russia
[§]Vaccine Research Center, National Institute of Allergy and Infectious Diseases, National Institutes of Health, Bethesda, Maryland 20892, United States

Ⓢ *Supporting Information*

ABSTRACT: The CD4 binding site on HIV-1 gp120 has been validated as a drug target to prevent HIV-1 entry to cells. Previously, we identified two small molecule inhibitors consisting of a 2,2,6,6-tetramethylpiperidine ring linked by an oxalamide to a *p*-halide-substituted phenyl group, which target this site, specifically, a cavity termed "Phe43 cavity". Here we use synthetic chemistry, functional assessment, and structure-based analysis to explore variants of each region of these inhibitors for improved antiviral properties. Alterations of the phenyl group and of the oxalamide linker indicated that these regions were close to optimal in the original lead compounds. Design of a series of compounds, where the tetramethylpiperidine ring was replaced with new scaffolds, led to improved antiviral activity. These new scaffolds provide insight into the surface chemistry at the entrance of the cavity and offer additional opportunities by which to optimize further these potential-next-generation therapeutics and microbicides against HIV-1.
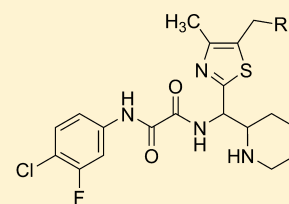
R = OH; **27**; TZM-bl cells, IC$_{50}$ = 1.60 μM

R = CH$_2$OH; **39**; TZM-bl cells, IC$_{50}$ = 1.98 μM

■ INTRODUCTION

Human immunodeficiency virus type-1 (HIV-1) is the etiological agent responsible for the AIDS pandemic. According to 2011 UNAIDS report, 34 million people are living with HIV worldwide, a rise of 17% compared to 2001. However, the availability of low cost highly active antiretroviral therapies (HAART) has helped to lower the rate of new infection and death. Despite the success, emergence of resistance to the available drugs is a major problem, which justifies continuous search for novel drugs against this virus.

The first step in HIV life cycle is the entry/fusion of the virus to the target cells. The envelope glycoprotein gp120 initiates this process by binding to the cellular receptor CD4 on cell surface. This binding induces substantial structural rearrangement in gp120 which is required for its subsequent binding to cellular chemokine receptor CXCR4 or CCR5.[1,2] This interaction helps to expose the fusion domain of gp41 that initiates fusion and the entry of the virus to the host cells. Although all these steps are legitimate targets for developing entry inhibitors, only drugs targeting gp41[3,4] and CCR5[5] have been successfully developed and clinically available. The X-ray structure of gp120 bound to CD4 and the fragment of an antibody (Fab) 17b was solved in 1998.[6] The structure reveals that phenylalanine at position 43 (Phe43) binds to the vestibule of a cavity of gp120, termed "Phe43 cavity", and makes major hydrophobic contacts. This hydrophobic contribution accounts for 28% of the contact interactions between CD4 and gp120

residues; however, another residue, arginine 59 (Arg59) of CD4, also makes critical interaction by forming a salt bridge with aspartic acid residue at position 368 (Asp368) of gp120. In addition, gp120 residues in the span of 365−371 and 425−430 contribute to about 58% of the interactions.[6] Several hydrophobic residues in those two regions are critical and make hydrophobic contacts with the hydrophobic residues in CD4. Insertions into this cavity were found to enhance the affinity of CD4 and of CD4-mimetics,[7] and we were the first to identify small molecule inhibitors, NBD-556 (**1**) and NBD-557 (**2**)[8] (Figure 1), which appear to insert into the "Phe43 cavity".[9,10] These two compounds show low micromolar potency against several laboratory strains and primary isolates. In addition, these molecules induce conformational changes in gp120 similar to CD4.[11] Recently, we cocrystallized **1** with the clade C strain C1086 version of gp120 core$_e$.[12] The structure reveals that **1** binds within the "Phe43 cavity" of gp120 with its 4-chlorophenyl group extended deep inside the cavity surrounded by hydrophobic residues, such as Trp112, Val255, Trp427, and Met475. The distal NH of the oxalamide group from 4-chlorophenyl ring forms an H-bond with Gly473. However, no apparent interaction of the tetramethylpiperidine ring with any residues in the cavity was observed; rather it was exposed outside of the pocket. The structural insight led us (this

1 (NBD-556); R = Cl
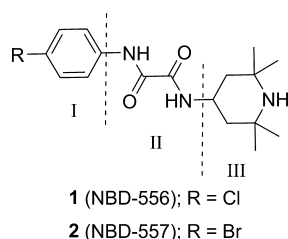**2** (NBD-557); R = Br

Figure 1. Structures of **1** and **2** identifying different pharmacophoric regions.

manuscript) and others to believe that the tetramethylpiperidine moiety can be replaced with other groups that may be able to take advantage of additional interactions, especially with Asp368, near the entrance of the cavity and yield more potent antivirals.[9,13,14]

In this report, we present the systematic modification of **1** to more potent inhibitors using structure-based design, synthesis, antiviral screening, and structure−activity relationship analyses. Our data indicate that structure-guided modifications, especially of region III with new scaffolds never reported before, improved the activity of several analogues by ~6-fold compared to **1**.

■ RESULTS AND DISCUSSION

Virtual Screening To Identify New Scaffolds To Replace 2,2,6,6-Tetramethylpiperidine Ring. We initiated a strategy for designing next generation entry inhibitors targeted to "Phe43 cavity" based on our earlier identified small molecule CD4-mimetics **1**[8] (Figure 1) and the X-ray structure of **1** bound to HIV-1 gp120 core. In our initial attempt for a limited structure−activity relationship (SAR) study on **1** we wanted to extend the hydrophobic portion of the oxalamide chain in region II (Figure 1) as defined by Lalonde et al.[14] and designed several succinamide containing compounds (Supporting Information). However, these compounds failed to show any antiviral activity in both single-cycle and multicycle inhibition assay. Recently, Lalonde et al also reported similar observation when testing a succinamide

analogue of **1**.[14] In addition, we (this report) and Lalonde et al. observed that variations of the oxalamide chain resulted in either poor activity or no antiviral activity at all.[14] Therefore, we turned our attention to modify the 2,2,6,6-tetramethylpiperidine ring. The structural insights described before motivated us to replace the 2,2,6,6-tetramethylpiperidine ring with other scaffolds that may provide a similar interaction as was observed between Arg59 and Asp368 as well as interact with other available binding residues. Since **1** was prepared by simple coupling reaction between 2-(4-chlorophenylamino)-2-oxoacetyl chloride and 4-amino-2,2,6,6-tetramethylpiperidine, we first identified 208 commercially available amines with diverse structures to replace the tetramethylpiperidine part and created a virtual library with 33 anilines consisting of 6864 compounds. Besides 4-chloroaniline, we also used a variety of substituted anilines to investigate how they fit in the "Phe43 cavity". The structure of the compounds in the virtual library was in 2D format; therefore, we used the LigPrep module within Maestro (Schrodinger, San Diego, CA) to generate 3D structures. The LigPrep module not only converts 2D structure to 3D but also considers tautomeric, stereochemical, and ionization states of the structure and generates conformations and performs energy minimization. The LigPrep application generated 20 688 structures representing all tautomeric, stereochemical, and ionization states of the molecules. We then performed a GLIDE-based docking[15,16] of these structures using the standard precision (SP) mode and selected 500 best scored structures to dock again using the extra precision (XP) scoring mode. We selected 50 top scored structures from this simulation. However, it is worth mentioning that within the top 50 structures the same molecule appeared multiple times because of different stereochemical, tautomeric, and ionization states. We noticed that the top XP scored molecule (−8.8) and several others within the top 50 molecules contained (2-(amino)piperidine-2-yl)methyl)-4-methylthiazolyl-5-yl)-methanol scaffold with variable substitutions in the phenylamine moiety. Another major observation was that the positively charged piperidine ring of the scaffold formed a salt bridge with Asp368 of gp120 (Figure 2). This interaction was
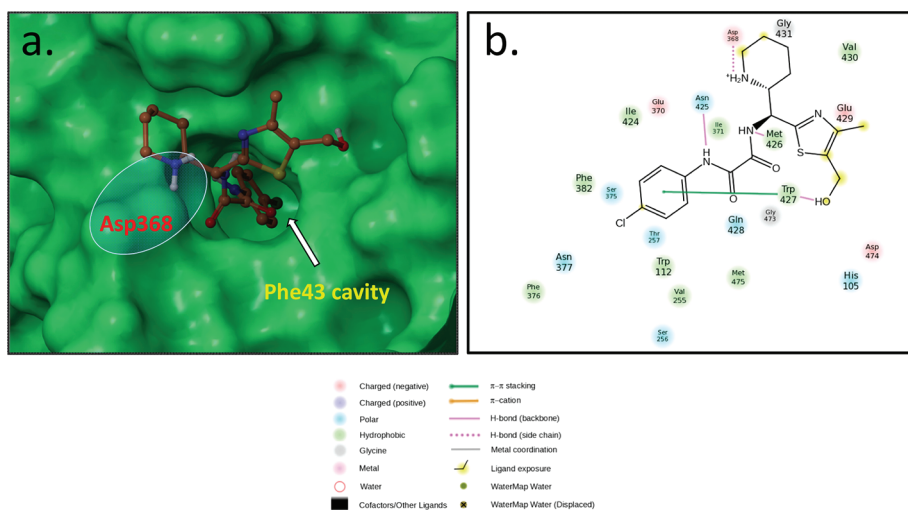
Figure 2. GLIDE-based docking of compound **6** in the "Phe43 cavity". (a) Compound **6** is shown as docked inside the cavity. The 4-chlorophenyl moiety is located deep inside the cavity. The protonated "N" of piperidine ring is within salt-bridge (H-bond interaction) distance from Asp368. (b) Shown are the interactions of **6** with the residues in the "Phe43 cavity" of HIV-1 gp120 as mapped by the Maestro software in Schrödinger Suite 2011.

Scheme 1[a]
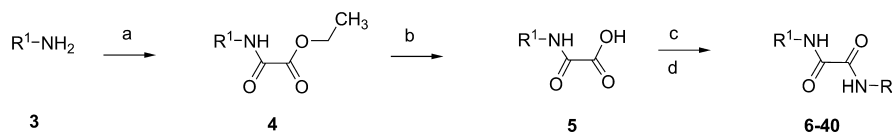
R[1] = Substituted anilines and aromatic amines as shown in Table-1 and 2; R = Primary amines as shown in Table-1

[a]Reagents: (a) ClCOCOOEt, NEt$_3$, DCM; (b) NaOH, EtOH, H$_2$O; (c) TBTU, NEt$_3$, amine; (d) HCl/dioxane (this step is only required to deprotect *N*-Boc amines).

absent in most of the other top scored compounds. Since we wanted to capture this interaction in our newly designed compounds, we decided to use this scaffold and its structural variations as the main target for synthesis.

Initially, we restricted our synthesis effort using 4-chlorophenylamine in region I (Figure 1) because of the fact that we observed earlier that the phenyl moiety could tolerate limited substitutions and 4-chloro was the most active so far. We also selected a few other top scored compounds for synthesis that did not satisfy the salt-bridge formation to compare their activity; however, we needed to make some minor changes because of the lack of availability of the exact reagents that were used to create the virtual library (Table 2). All these compounds with the variations were docked using the same method and inspected for their fit in the Phe43 cavity. All of them fit very well as the original scaffold with high score (>−7.0).
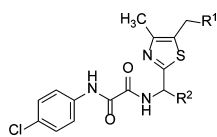
Chemistry. The oxalamide derivatives were prepared by adopting the general procedure in Scheme 1. This allows probing different haloaryl derivatives in region I and virtually any kind of available amine in region III (Figure 1). A series of commercially available arylamines (Tables 1 and 2 and Table S1) have been coupled with the ethyl 2-chloro-2-oxoacetate (a). The resulting intermediate was hydrolyzed (b) and coupled with commercially available amines (c) (Tables 1 and 2 and Table S1). When Boc-protected amines were used, an additional step of cleaving was necessary (d). The resulting coupling product was HPLC purified and characterized by ^{1}H NMR and LC−MS. Some of the reported compounds were isolated as a diastereoisomeric mixture with variable purity. No further attempt was made to separate the individual isomer at this stage.

Structure−Activity Relationship (SAR). In our initial attempt to understand the SAR we decided to explore few compounds by replacing the oxalamide moiety in region II of our earlier reported compounds, **1**, with succinamide (Table S1 in Supporting Information). No docking-based selection method was used. Rather those compounds were synthesized based on reagent availability. However, none of the compounds showed any noticeable antiviral activity either in single-cycle or in multicycle assay. On the basis of the docking simulation, the best XP-scored compound had the 4-bromo-3-fluorophenyl moiety (Figure S1). However, we decided initially to explore the 4-chloroaniline based on our earlier reported compound **1**. Therefore, we synthesized the compound, NBD-09027 (**6**), and it showed low micromolar potency with good selectivity index (SI) in both single-cycle (in TZM-bl cells) and multicycle (in MT-2 cells) assays. Therefore, we concentrated our attention to understand the SAR of the piperidine ring of our initial best hit, **6**. Then we synthesized two additional compounds by moving the nitrogen from position 2 in the initial hit to positions 3 (**7**) and 4 (**8**). Both compounds showed substantial improvement

in antiviral activity in a single-cycle pseudovirus based assay. In addition, the toxicity in TZM-bl cells also decreased remarkably. Unfortunately, both compounds were much less active in MT-2 cell based multicycle infectivity assay. A similar study was done with our follow-up most active compound NBD-10007 (**9**). Again we observed remarkable improvement in antiviral potency as well as toxicity for both **10** and **11** in the TZM-bl based pseudovirus assay. However, both compounds again showed much lower potency in MT-2 based infectivity assay. Since these two assay methods are different and different cells were used, some variations in activity were expected. However, no clear SAR could be discerned from the multicycle infectivity based antiviral data. Recently, a multicenter comparison study of HIV neutralization assay indicated that pseudovirus assays are generally more sensitive than multicycle virus inhibition assay; however, it also depends on the virus and inhibitor used.[17] The presence of either hydroxymethanol or hydroxyethanol on the thiazole ring did not make any appreciable differences in antiviral activity. These groups most likely work as the solubilizing unit of these molecules instead of conferring any direct binding. Next, we have substituted H of the NH of the piperidine ring with methyl (**12**) and acetyl (**13**). The antiviral activity of methyl substituted piperidine (**12**) improved compared to its unsubstituted counterpart (**9**), but the toxicity level remained the same. The acetyl substituted piperidine analogue (**13**) showed much worse activity, but the toxicity improved substantially. In both cases, the antiviral activity in MT-2 cells was poor, as was observed with unsubstituted analogues. Complete removal of the piperidine ring with the methylaminoethyl (−CH$_2$NHCH$_3$) moiety also showed potent antiviral activity in single-cycle pseudovirus-based assay but showed poor activity in MT-2 cell based multicycle infectivity assay. Again, the toxicity of this analogue was high. We also tested three structurally diverse analogues (**17**−**19**), but they either had poor activity or no activity at all in both infectivity assays.
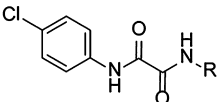
Since **6** and **9** showed much better activity profile in both assays, we restricted our synthesis effort in designing analogues based only on these two active inhibitors. This time, we focused our attention mostly to include substitutions to the phenyl ring (Table 2). Substituting 4-Cl with CF$_3$ (**20**) resulted in somewhat reduced antiviral activity. When the acetyl group was introduced at the para position of the phenyl ring (**23**), the compound became totally inactive. The introduction of a smaller substituent (F) at the ortho position of the phenyl ring was found to be detrimental to the antiviral activity (**21**). However, interestingly, 4-Cl and 4-CH$_3$ groups with 3-F (**27**, **28**, **38**, and **39**) in both −CH$_2$OH and −CH$_2$CH$_2$OH substituted thaizoles showed much improved activity. This is consistent with the observation reported with 2,2,6,6-tetramethylpiperidine containing compounds[9] and recently with a large number of compounds where 4-amino-2,2,6,6-
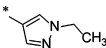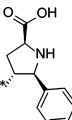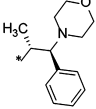
Table 1. Structure and Antiviral Activity of Oxalamide Series Compounds in Single-Cycle (TZM-bl) and Multicycle (MT-2) Inhibition Assays

No	R[1]	R[2]	TZM-bl cells		MT-2 Cells	
			IC$_{50}$ (µM ± SD)	^{a}CC$_{50}$ (µM ± SD)	IC$_{50}$ (µM ± SD)	^{a}CC$_{50}$ (µM ± SD)
6	OH	piperidin-2-yl	4.3 ± 1.0	>22 (10%)	4.7 ± 0.6	>108 (40%)
7	OH	piperidin-3-yl	1.4 ± 0.4	~60.2	12 ± 1.1	>81
8	OH	piperidin-4-yl	0.83 ± 0.14	~81	29.8 ± 3.5	>81
9	CH$_2$OH	piperidin-2-yl	4.6 ± 0.7	32.8 ± 0.6	4.2 ± 0.2	>62 (0%)
10	CH$_2$OH	piperidin-3-yl	0.65 ± 0.1	~59.4	13.1 ± 2.4	>78.5
11	CH$_2$OH	piperidin-4-yl	1.0 ± 0.8	~85.4	30.5 ± 3.4	>78.5
12	CH$_2$OH	1-methylpiperidin-2-yl	1.9 ± 0.25	36 ± 3.3	28.6 ± 1.6	~88
13	CH$_2$OH	1-acetylpiperidin-2-yl	19.7 ± 1.3	>84 (20%)	>52	>84
14	OH	pyrrolidin-2-yl	4.8 ± 0.5	12.4 ± 0.7	15.4 ± 2.6	~45
15	CH$_2$OH	pyrrolidin-2-yl	4.2 ± 0.3	~4.9	16.2 ± 1.7	~42
16	CH$_2$OH	CH$_2$NHCH$_3$	2.8 ± 0.3	16.6 ± 1.0	24.3 ± 2.2	>43

Table 1. continued

No	R	TZM-bl cells		MT-2 Cells	
		IC$_{50}$ (µM ± SD)	^{a}CC$_{50}$ (µM ± SD)	IC$_{50}$ (µM ± SD)	^{a}CC$_{50}$ (µM ± SD)
17		5.9 ± 0.4	~8	11.9 ± 1.2	10.7 ± 1.6
18		>99.6	>99.6	>24.9	>99.6
19		>99.6	>99.6	>24.9	>99.6
1		4.2 ± 0.5	>60 (10%)	8 ± 0.2	~150

^{a}The number in parentheses indicates % toxicity at that dose.

tetramethylpiperidine was replaced by diverse amines.[14] In a more drastic move we have replaced the phenyl ring with a seven-membered alicyclic ring, and those compounds (**29** and **40**) showed no antiviral activity. This confirms our earlier observation that the phenyl ring can only accommodate limited substitutions because of the narrow hydrophobic pocket in the "Phe43 cavity".

To understand the expected binding mode of two of the most active compounds that contained 4-Cl with 3-F substituents in the phenyl rings NBD-11009 (**27**) and NBD-11018 (**39**), we performed GLIDE-based docking simulations in XP mode as described before. The top scoring conformations of these two inhibitors indicated two possible binding modes (Figure 3). In both cases, the 4-Cl-3-F-phenyl ring was surrounded by hydrophobic residues similar to what we observed with **6**; however, there was considerable difference between two binding modes of the piperidinethiazolyl moiety of **27** (Figure 3 a,b). Surprisingly, the positively charged piperidine nitrogen of the top scored (−8.22) **27** conformation did not form any H-bond/salt-bridge with Asp368, whereas in the next best scored (−7.89) conformation it indeed formed the H-bond/salt-bridge with Asp368. In both cases the −CH$_2$OH formed H-bond with Trp427. On the contrary, the positively charged piperidine nitrogen in both top scored (−7.96) and the next best scored (−7.81) conformations of **39** formed H-bond/salt-bridge with Asp368 (Figure 3c,d). This difference in the binding mode may be attributed to the larger size of the ethanol moiety on the thiazole ring. However, the −CH$_2$CH$_2$OH group had different binding modes in two different conformations. One noticeable feature was that in all these conformations the oxalamide moiety had the same

interaction. One of its NH attached to the phenyl ring formed an H-bond with Asn425. This is somewhat different from what we observed with **6** (Figure 2) where in addition to the same H-bond the distal NH of the oxalamide linker also formed an H-bond with Met426. This predicted binding information is expected to guide future optimization of this class of inhibitors.

■ CONCLUSIONS

After our first discovery of two small molecule inhibitors that target the "Phe43 cavity" in 2005, it has been conclusively shown that these compounds bind to the cavity with remarkable ability to alter the conformation of gp120 similar to that observed when CD4 bound to gp120. This extraordinary ability of these small molecules resulted in solving the crystal structures of these molecules with gp120, which provided details of the binding mode of these compounds in the cavity. Despite many attempts by us and others using traditional medicinal chemistry, the 2,2,6,6-tetramethylpiperidine ring could not be replaced successfully by any other chemical scaffold until this report to improve the antiviral activity. In fact, all attempts reported until recently[14] indicate failure to obtain compounds with activity better than **1** and **2** . In this study, we have successfully utilized the structural insights of the X-ray crystal structure of **1** bound to gp120 to design a large number of molecules with new scaffold replacing the 2,2,6,6-tertamethylpiperidine ring. Several of these new compounds showed improved potency in single-cycle as well as multicycle HIV-1 inhibition assays. The most notable achievement is the identification of new scaffolds which should provide opportunities to optimize these compounds further. Since these compounds prevent HIV-1 from entering cells, they may serve
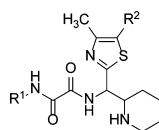
Table 2. Structure−Activity Relationship (SAR) Analysis of Oxalamide Compounds in Single-Cycle (TZM-bl) and Multicycle (MT-2) Assays

No	R¹	R²	TZM-bl cells		MT-2 Cells	
			IC$_{50}$ (µM ± SD)	^{a}CC$_{50}$ (µM ± SD)	IC$_{50}$ (µM ± SD)	^{a}CC$_{50}$ (µM ± SD)
6	Cl—⟨ ⟩—*	*−CH$_2$OH	4.3 ± 1.1	>22 (10%)	4.7 ± 0.6	>108 (40%)
20	F$_3$C—⟨ ⟩—*	*−CH$_2$OH	10.3 ± 1.6	>75.5 (10%)	4.6 ± 0.3	>75.5
21	F—⟨ ⟩—* (F)	*−CH$_2$OH	>87	>87	~110	>110
22	F—⟨ ⟩—* (F)	*−CH$_2$OH	8.4 ± 2.0	>87 (0%)	14 ± 3.8	>87
23	H$_3$C–C(O)—⟨ ⟩—*	*−CH$_2$OH	>86	>86	~107	>107
24	F—⟨ ⟩—* (Cl)	*−CH$_2$OH	6.5 ± 1.0	>77.8 (0%)	9.5 ± 1.4	>77.8
25	F—⟨ ⟩—*	*−CH$_2$OH	7.4 ± 0.4	>90 (0%)	47.9 ± 5.5	>113
26	H$_3$C—⟨ ⟩—* (F)	*−CH$_2$OH	>88	>88	~66	>109
27	Cl—⟨ ⟩—* (F)	*−CH$_2$OH	1.6 ± 0.07	~58.4	3.8 ± 0.7	~77.8
28	H$_3$C—⟨ ⟩—* (F)	*−CH$_2$OH	2.7 ± 0.41	>88 (0%)	5.3 ± 0.5	>88 (30%)
29	⟨cycloheptyl⟩—*	*−CH$_2$OH	>90	>90	39.3 ± 5	>90
30	Cl—⟨ ⟩—*	*−CH$_2$CH$_2$OH	4.6 ± 0.7	32.8 ± 0.6	4.2 ± 0.3	>62 (0%)
31	F$_3$C—⟨ ⟩—*	*−CH$_2$CH$_2$OH	4.9 ± 0.5	>74 (35%)	17.4 ± 5.7	>39
32	F—⟨ ⟩—* (F)	*−CH$_2$CH$_2$OH	>84	>84	>105	>105
33	F—⟨ ⟩—* (F)	*−CH$_2$CH$_2$OH	8.2 ± 0.5	>78.2 (10%)	24.1 ± 4.6	>78.2
34	H$_3$C–C(O)—⟨ ⟩—*	*−CH$_2$CH$_2$OH	>77.3	>77.3	24.5 ± 1.5	>48.3
35	F—⟨ ⟩—* (Cl)	*−CH$_2$CH$_2$OH	9.0 ± 1.0	>75.8 (20%)	19.5 ± 1.8	~94.7
36	F—⟨ ⟩—*	*−CH$_2$CH$_2$OH	~22	>88	21.6 ± 3.5	~109
37	H$_3$C—⟨ ⟩—* (F)	*−CH$_2$CH$_2$OH	>78.8	>78.8	45.8 ± 3.5	>78.8
38	H$_3$C—⟨ ⟩—* (F)	*−CH$_2$CH$_2$OH	1.66 ± 0.06	>85 (40%)	3.7 ± 0.7	~85
39	Cl—⟨ ⟩—* (F)	*−CH$_2$CH$_2$OH	1.98 ± 0.19	~61	3.5 ± 0.9	>41 (10%)
40	⟨cycloheptyl⟩—*	*−CH$_2$CH$_2$OH	>88	>88	19.6 ± 4	~60

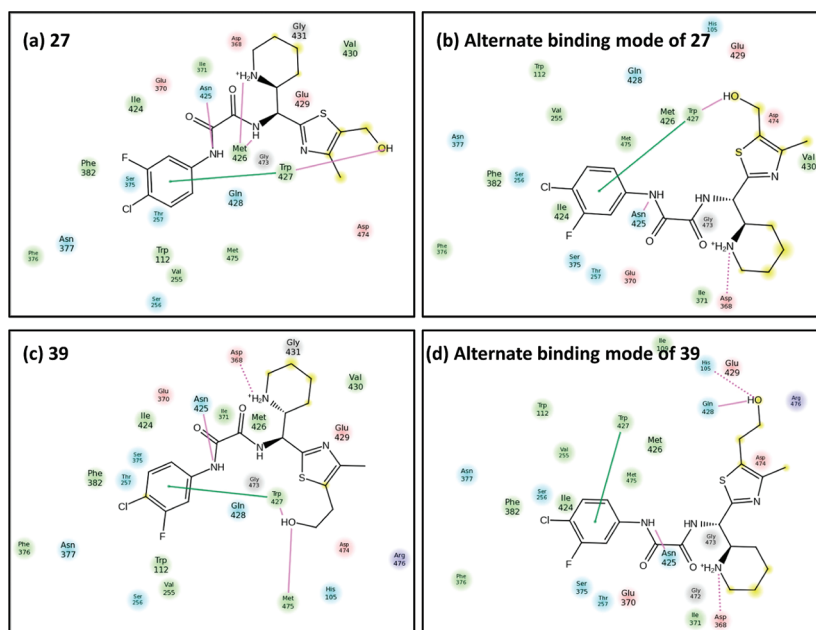^{a}The number in parentheses indicates % toxicity at that dose.

Figure 3. Binding mode of two of the most active compounds, **27** and **39**. (a, b) The docking-based top scoring two conformations of **27** showed distinct differences in binding of the piperidinethiazolyl moiety. The piperidine NH formed an H-bond/salt-bridge with Asp368 in the second best scored conformation but not in the top scored conformation. (c, d) Both top scored two conformations of **39**, on the other hand, formed the H-bond/salt-bridge with Asp368. However, the ethanol moiety in the thiazolyl ring showed two distinct binding modes. The symbol notations are same as in Figure-2.

Scheme 2[a]
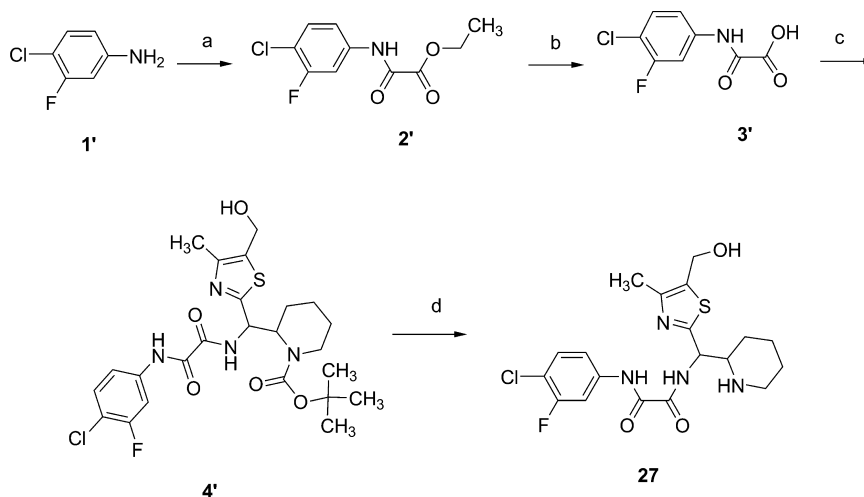
[a]Reagents: (a) ClCOCOOEt, NEt$_3$, DCM; (b) NaOH, EtOH, H$_2$O; (c) TBTU, NEt$_3$, amine; (d) HCl/dioxane.

as potential leads to develop next-generation therapeutics and microbicides against HIV-1.

EXPERIMENTAL SECTION

All reagents were purchased from commercial suppliers or obtained in-house (Asinex) and were used without further purification. The melting points were measured on a Sanyo Gallenkamp melting point apparatus (Sanyo Gallenkamp, U.K.). The LC−MS analyses for the compounds were done at Surveyor MSQ (Thermo Finnigan, U.S.) with APCI ionization. The ^{1}H NMR spectra were recorded on Mercury Plus 400 MHz spectrometer (Varian, Germany). Chemical shift values are given in ppm relative to tetramethylsilane (TMS), with the residual solvent proton resonance as internal standard. High-resolution mass spectra were recorded on a Bruker APEX II ICR-FTMS. Purity of compounds was determined by HPLC. Purity of

compounds were ≥95% unless otherwise mentioned. HPLC analyses were performed on a Water XTerra MS C18 analytical column (2.1 mm × 30 mm, particle size 3.5 μm) using DMSO/acetonitrile (50:50), at a flow rate of 15 mL/min at 25 °C. The oxalamide compounds were isolated as diastereoisomers with variable isomer ratios.

MT-2 cells (human T-cell leukemia cells, obtained through the AIDS Research and Reference Reagent Program from Dr. D. Richman.) were grown in RPMI 1640 medium (Gibco) supplemented with 10% fetal bovine serum (FBS), penicillin, and streptomycin (100 U/μL each). TZM-bl cells (a HeLa cell line that expresses CD4, CXCR4, and CCR5 and expresses luciferase and β-galactosidase under control of the HIV-1 promoter, obtained from Dr. John C. Kappes, Dr. Xiaoyun Wu, and Tranzyme Inc.) and 293T cells (ATCC) were grown in Dulbecco's modified Eagle's medium (DMEM) (Gibco) supplemented with 10% FBS, penicillin, and streptomycin. pNL4-3.Luc.R-E-DNA was obtained through the AIDS Research and Reference

Reagent Program from Dr. N. Landau and env expression vector pHXB2-env (X4) DNA from Dr. K. Page and Dr. D. Littman.[18]

Virtual Screening Using GLIDE-Based Docking. We used the automated docking software GLIDE 5.7 (Schrödinger, Portland, OR) within Schrödinger Suite 2011 that applies a two-stage scoring process to sort out the best conformations and orientations of the ligand (defined as pose) based on its interactions with the receptor. GLIDE has been used successfully in drug design.[19−25] We used our recently solved X-ray crystal structure of **1** with the clade C strain C1086 version of gp120 core$_e$ at 2.7 Å resolution for docking simulations (PDB code 3TGS).[12] Three-dimensional coordinates of the ligands and their isomeric, ionization, and tautomeric states were generated using the LigPrep (including Ionizer) module within the Schrödinger Suite 2011 programs. The protein was prepared using the "protein preparation tool", and the structures were minimized with Macromodel software within Schrödinger Suite 2011. A grid file encompassing the area in the cavity that contains information on the properties of the associated receptor was created. Conformational flexibility of the ligands was handled via an exhaustive conformational search. Initially, we used Schrödinger's proprietary GlideScore scoring function in standard precision (SP) mode. We selected 500 top-scored compounds to dock again in extra precision (XP) mode to score the optimized poses. The 50 top-scored ligands were selected from this simulation for further study.

Synthesis of Oxalamide Series, Compounds 6−40. Since the compounds from the oxalamide series were synthesized according to general Scheme 1, we presented a representative synthesis (Scheme 2) of one of the most active compounds (**27**) from Table 2, and all other compounds in this series were synthesized by following this method. The deprotection step (d) was only used when *N*-Boc protected amines were used as described below.

Ethyl 2-(4-Chloro-3-fluorophenylamino)-2-oxoacetate (2′). TEA (2.28 g, 0.023 mol) was added at once to a solution of 3 g (0.0206 mol) of 4-chloro-3-fluoroaniline in 50 mL of DCM, and then ethyl 2-chloro-2-oxoacetate (2.81 g, 0.0206 mol) was added dropwise at 0 °C. The reaction mixture was stirred at 0 °C for 1 h and then at room temperature for 6 h. The mixture was washed with 25% aqueous solution of K_2CO_3 (2 × 50 mL) and water (50 mL). The product was dried over Na_2SO_4 and evaporated. The residue was washed with ether and dried in air to give ethyl 2-(4-chloro-3-fluorophenylamino)-2-oxoacetate (**2′**) (3.97 g, 78.6%) as a white powder. LC−MS (APCI$^+$) *m/z*: calcd for $C_{10}H_9ClFNO_3$, 245.03; found, 245 (M + H$^+$).

2-(4-Chloro-3-fluorophenylamino)-2-oxoacetic Acid (3′). Ethyl 2-(4-chloro-3-fluorophenylamino)-2-oxoacetate (4.18 g, 0.017 mol) was added to a solution of NaOH (1.361 g, 0.0340 mol) in a mixture 50 mL of EtOH and 50 mL of water, and the resulting mixture was stirred at room temperature for 6 h. The mixture was acidified with 2 N HCl to pH 4−5 at 0 °C. The precipitate was filtered, washed with water, and dried in air to afford 2-(4-chloro-3-fluorophenylamino)-2-oxoacetic acid (**3′**) (2 g, 55.2%) as a white solid. LC−MS (APCI$^+$) *m/z*: calcd for $C_8H_5ClFNO_3$, 216.99; found, 217 (M + H$^+$).

***tert*-Butyl 2-((2-(4-Chloro-3-fluorophenylamino)-2-oxoacetamido)(5-(hydroxymethyl)-4-methylthiazol-2-yl)methyl)piperidine-1-carboxylate (4′).** A mixture of 2-(4-chloro-3-fluorophenylamino)-2-oxoacetic acid (**3′**) (0.3 g, 1.378 mmol), TBTU (0.530 g 1.65 mmol), and TEA (0.166 g, 1.65 mmol) in DCM (20 mL) was stirred at room temperature for 1 h. Then 2-[amino-(5-hydroxymethyl-4-methylthiazol-2-yl)methyl]piperidine-1-carboxylic acid *tert*-butyl ester (0.470 g, 1.378 mmol) was added, and stirring was continued for 6 h. The reaction mixture was washed with 25% aqueous solution of K_2CO_3 (2 × 50 mL) and water (50 mL). The product was dried over Na_2SO_4 and evaporated. The residue was purified by column chromatography on silica gel (EtOAc/hexane, 1/1) to afford *tert*-butyl 2-((2-(4-chloro-3-fluorophenylamino)-2-oxoacetamido)(5-(hydroxymethyl)-4-methylthiazol-2-yl)methyl)piperidine-1-carboxylate (**4′**) (0.53 g, 72%) as a white solid. LC−MS (APCI$^+$) *m/z*: calcd for $C_{24}H_{30}ClFN_4O_5S$, 540.16; found, 541 (M + H$^+$).

N^1-(4-Chloro-3-fluorophenyl)-N^2-((5-(hydroxymethyl)-4-methylthiazol-2-yl)(piperidin-2-yl)methyl)oxalamide·2HCl (27). *tert*-Butyl 2-((2-(4-chloro-3-fluorophenylamino)-2-oxoacetami-do) (5-(hydroxymethyl)-4-methylthiazol-2-yl)methyl)piperidine-1-car-boxylate (**4′**) (0.250 g, 0.462 mmol) was dissolved in dioxane (20 mL), and 15% solution HCl in dioxane (20 mL) was added. The resulting mixture was stirred at room temperature for 6 h. Solvent was distilled off and residue was triturated with acetone/ether to give N^1-(4-chloro-3-fluorophenyl)-N^2-((5-(hydroxymethyl)-4-methylthiazol-2-yl)-(piperidin-2-yl)methyl)oxalamide hydrochloride (**27**) (0.114 g, 52%) (diastereoisomeric mixture, 1:5). LC−MS (APCI$^+$) *m/z*: calcd for $C_{19}H_{22}ClFN_4O_3S$, 440.11; found, 441 (M + H$^+$), 443.15 (M$^+$ + 2), 444.15. HPLC: >92%. ^{1}H NMR (DMSO-d_6, 50 °C, 400 MHz) δ_H, 1.32−1.75 (m, 6H, C$\underline{H}_2$), 2.27 (s, 3H, -C$\underline{H}_3$), 2.75−3.00 (m, 1H, C$\underline{H}_2$-N), 3.27 (m, 1H, C$\underline{H}_2$-N), 3.80 (m, 1H, C$\underline{H}$-N), 4.56 (s, 2H, -C$\underline{H}_2$-OH), 5.38 (t, 1H for one isomer, C$\underline{H}$-), 5.51 (t, 1H for the other, C$\underline{H}$-), 6.00−6.30 ($\underline{H}_2$O + $\underline{H}^+$ + -O$\underline{H}$ signals), 7.51 (t, 1H, Ar$\underline{H}$-), 7.59 (d, 1H, Ar$\underline{H}$-), 7.87 (d, 1H, Ar$\underline{H}$t-), 8.50−9.50 (m br, 2H, N$\underline{H}_2^+$), 9.53 (br, 1H, CON$\underline{H}$), 11.00 (s, 1H for one isomer, CON$\underline{H}$), 11.09 (s, 1H for the other, CON$\underline{H}$).

N^1-(4-Chlorophenyl)-N^2-((5-(hydroxymethyl)-4-methylthia-zol-2-yl)(piperidin-2-yl)methyl)oxalamide·HCl (6). White solid. Yield: 42% (diastereoisomeric mixture, 1:1). LC−MS (APCI$^+$) *m/z*: calcd for $C_{19}H_{23}ClN_4O_3S$, 422.12; found, 422.98 (M + H$^+$). HPLC: 95.8%. ^{1}H NMR (DMSO-d_6, 50 °C, 400 MHz) δ_H, 1.32−1.90 (m, 6H), 2.27 (s, 3H, -C$\underline{H}_3$), 2.75−3.00 (m, 1H), 3.33, (m, 1H), 3.80 (m, 1H), 4.56 (s, 2H, -C$\underline{H}_2$-OH), 5.38 (t, 1H for one isomer), 5.51 (t, 1H for the other), 7.40 (d, 2H), 7.84 (d, 2H), 8.50−9.30 (m br, 2H, N$\underline{H}_2^+$), 9.61 (d, 1H for one isomer, N$\underline{H}$), 9.68 (d, 1H for the other, N$\underline{H}$), 11.80 (s, 1H for one isomer, CON$\underline{H}$), 10.91 (s, 1H for the other, CON$\underline{H}$).

N^1-(4-Chlorophenyl)-N^2-((5-(hydroxymethyl)-4-methylthia-zol-2-yl)(piperidin-3-yl)methyl)oxalamide·2HCl (7). White solid. Yield: 50% (diastereoisomeric mixture, 1:1). LC−MS (APCI$^+$) *m/z*: calcd for $C_{19}H_{23}ClN_4O_3S$, 422.12; found, 423.26 (M + H$^+$). HPLC: > 97.5%. ^{1}H NMR (DMSO-d_6, 50 °C, 400 MHz) δ_H, 1.34 (m, 1H), 1.65 (br, 1H), 1.82 (m, 2H), 2.27 (s, 3H, -C$\underline{H}_3$), 2.55 (m, 1H), 2.75 (m, 2H, -C$\underline{H}_2$-NH), 3,15 (m, 2H, -C$\underline{H}_2$-NH), 4.56 (s, 2H, -C$\underline{H}_2$-OH), 5.08 (m, 1H), 7.40 (d, 2H, Ar-$\underline{H}$), 7.83 (d, 2H, Ar-$\underline{H}$), 8.80 (br, 1H, N$\underline{H}_2^+$), 9.30 (br d and d, 1H, N$\underline{H}_2^+$), 9.50 (d and d, 1H, CON$\underline{H}$), 10.75 (s, 1H, CON$\underline{H}$).

N^1-(4-Chlorophenyl)-N^2-((5-(hydroxymethyl)-4-methylthia-zol-2-yl)(piperidin-4-yl)methyl)oxalamide·2HCl (8). White solid. Yield: 46% (single diastereoisomer). LC−MS (APCI$^+$) *m/z*: calcd for $C_{19}H_{23}ClN_4O_3S$, 422.12; found, 423.26 (M + H$^+$). HPLC: 95.0%. ^{1}H NMR (DMSO-d_6, 50 °C, 400 MHz) δ_H, 1.49 (br m, 2H), 1.68 (br d, 1H), 1.93 (br d, 1H), 2.26 (s, 3H, -C$\underline{H}_3$), 2,35 (br m, 1H), 2.80 (br m, 2H), 3.25 (br m, 2H), 3.55 (m, 1H), 4.56 (s, 2H, -C$\underline{H}_2$-OH), 4.68 (br t, 1H), 4.95 (m, 1H), 7.39 (d, 2H, Ar-$\underline{H}$), 7.83 (d, 2H, Ar-$\underline{H}$), 8.68 (br, 1H, N$\underline{H}_2^+$), 9.08 (br, 1H, N$\underline{H}_2^+$), 9.41 (d, 1H, CON$\underline{H}$), 10.78 (s, 1H, CON$\underline{H}$).

N^1-(4-Chlorophenyl)-N^2-((5-(2-hydroxyethyl)-4-methylthia-zol-2-yl)(piperidin-2-yl)methyl)oxalamide·HCOOH (9). White solid. Yield: 55% (diastereoisomeric mixture, 1:1). LC−MS (APCI$^+$) *m/z*: calcd for $C_{20}H_{25}ClN_4O_3S$, 436.13; found, 437.30 (M + H$^+$). HPLC: >95.0%. ^{1}H NMR (DMSO-d_6, 50 °C, 400 MHz) δ_H, 1.10−1.80 (m, 6H), 2.26 (s, 3H, -C$\underline{H}_3$), 2.75−3.00 (m, 3H), 3.00−3.80 (12H + NH + H_2O signal), 5.00 (br, 1H for one isomer), 5.10 (br, 1H for the other), 7.41 (d, 2H), 7.82 (d, 2H), 9.10 (br 1H for one isomer, N$\underline{H}_2^+$), 9.38 (br, 1H for the other, N$\underline{H}_2^+$), 10.85 (s, 1H, N$\underline{H}$).

N^1-(4-Chlorophenyl)-N^2-((5-(2-hydroxyethyl)-4-methylthia-zol-2-yl)(piperidin-3-yl)methyl)oxalamide·2HCl (10). White solid. Yield: 37% (diastereoisomeric mixture, 1:1). LC−MS (APCI$^+$) *m/z*: calcd for $C_{20}H_{25}ClN_4O_3S$, 436.13; found, 437.27 (M + H$^+$). HPLC: 98.2%. ^{1}H NMR (DMSO-d_6, 50 °C, 400 MHz) δ_H, 1.40 (m, 1H), 1.65 (br, 2H), 1.82 (m, 2H), 2.27 (s, 3H, -C$\underline{H}_3$), 2.55 (br, 1H), 2.65−2.88 (m, 4H), 3,13 (m, 2H), 3,55 (m, 2H, -C$\underline{H}_2$-C$\underline{H}_2$-OH), 5.07 (m, 1H), 7.39 (d, 1H, Ar-$\underline{H}$), 7.82 (d, 1H, Ar-$\underline{H}$), 8.75 (br, 1H, N$\underline{H}_2^+$), 9.11 (br, 1H for one isomer, N$\underline{H}_2^+$), 9.24 (br, 1H for the other, N$\underline{H}_2^+$), 9.48 (d, 1H for one isomer, CO-N$\underline{H}$), 9.51 (d, 1H for the other, CO-N$\underline{H}$), 10.75 (s, 1H, CO-N$\underline{H}$).

N^1-(4-Chlorophenyl)-N^2-((5-(2-hydroxyethyl)-4-methylthia-zol-2-yl)(piperidin-4-yl)methyl)oxalamide·2HCl (11). White

solid. Yield: 44% (single diastereoisomer). LC−MS (APCI$^+$) m/z: calcd for C$_{20}$H$_{25}$ClN$_4$O$_3$S, 436.13; found, 437.21 (M + H$^+$). HPLC: 95%. ^{1}H NMR (DMSO-d_6, 50 °C, 400 MHz) δ_H 1.45 (m, 2H), 1.68 (d, 1H), 1.95 (d, 1H), 2.25 (s, 3H, CH$_3$), 2.35 (m, 1H), 2.80 (m, 4H), 3.24 (m, 2H), 3,40−3.70(m, 3H), 4,95 (t, 1H,), 7.39 (d, 2H, Ar-H), 7.82 (d, 2H, Ar-H), 8.65 (br, 1H, NH$_2$$^+$), 8.88 (br, 1H, NH$_2$$^+$), 9.35 (d, 1H, CO-NH), 10.75 (s, 1H, CO-NH).

N^1-(4-Chlorophenyl)-N^2-((5-(2-hydroxyethyl)-4-methylthiazol-2-yl)(1-methylpiperidin-2-yl)methyl)oxalamide (12). White solid. Yield: 38% (single diastereoisomer). LC−MS (APCI$^+$) m/z: calcd for C$_{21}$H$_{27}$ClN$_4$O$_3$S, 450.15; found, 451.12 (M + H$^+$). HPLC: 93.0%. ^{1}H NMR (CDCl$_3$, 45 °C, 400 MHz) δ_H, 1.20−2.20 (m, 8H) 2.35(s, 3H, -CH$_3$), 2.38 (s, 3H, -CH$_3$), 2.71 (br, 1H, -CH-NMe), 2.95 (m, 4H, -CH$_2$-CH$_2$-OH), 3.80 (m, 2H, -CH$_2$-CH$_2$-OH), 5.10 (br, 1H, CONH-CH), 7.31 (d, 2H ArH,), 7.53 (d, 2H ArH,), 8.40 (br, 1H, CONH-CH) 9.28 (s, 1H, Ar-NHCO-).

N^1-((1-Acetylpiperidin-2-yl)(5-(2-hydroxyethyl)-4-methylthiazol-2-yl)methyl)-N^2-(4-chlorophenyl)oxalamide (13). White solid. Yield: 36% (single diastereoisomer). LC−MS (APCI$^+$) m/z: calcd for C$_{22}$H$_{27}$ClN$_4$O$_4$S, 478.14; found, 479.12 (M + H$^+$). HPLC: 90.0%. ^{1}H NMR (DMSO-d_6, 50 °C, 400 MHz) δ_H, 1.10−2.20 (m, 9H), 2.27 (s, 3H, -CH$_3$), 2.80 (m, 2H,), 3.56 (m, 2H, -CH$_2$-OH), 4.75, (m, 1H,) 5.12 (m, 1H), 5.48 (m, 1H,), 7.41 (d, 2H), 7.82 (d, 2H), 8.35 (br 1H, CO-NH), 10.75 (s, 1H, CO-NH).

N^1-(4-Chlorophenyl)-N^2-((5-(hydroxymethyl)-4-methylthiazol-2-yl)(pyrrolidin-2-yl)methyl)oxalamide·HCOOH (14). White solid. Yield: 39% (diastereoisomeric mixture, 1:1). LC−MS (APCI$^+$) m/z: calcd for C$_{18}$H$_{21}$ClN$_4$O$_3$S, 408.10; found, 409.28 (M + H$^+$). HPLC: 93.2%. ^{1}H NMR (DMSO-d_6, 50 °C, 400 MHz) δ_H, 1.40−1.90 (m, 4H, -CH$_2$-), 2.27 (s, 3H, -CH$_3$), 2.87 (m, 2H), 3.10−3.70 (NH + H$_2$O signal), (3.80 (m, 1H), 4.56 (s, 2, -CH$_2$-OH), 4.98 (br, 1H for one isomer), 5.08 (br, 1H for the other), 7.40 (d, 2H), 7.82 (d, 2H), 9.08 (br 1H for one isomer, NH$_2$$^+$), 9.40 (br, 1H for the other, NH$_2$$^+$), 10.85 (s, 1H, NH).

N^1-(4-Chlorophenyl)-N^2-((5-(2-hydroxyethyl)-4-methylthiazol-2-yl)(pyrrolidin-2-yl)methyl)oxalamide·HCOOH (15). White solid. Yield: 53% (diastereoisomeric mixture, 1:1). LC−MS (APCI$^+$) m/z: calcd for C$_{19}$H$_{23}$ClN$_4$O$_3$S, 422.12; found, 423.27 (M + H$^+$). HPLC: 95.0%. ^{1}H NMR (DMSO-d_6, 50 °C, 400 MHz) δ_H, 1.52 (m, 1H, -CH$_2$-), 1.69 (m, 2H, -CH$_2$-), 1.85 (m, 1H, -CH$_2$-) 2.27 (s, 3H, -CH$_3$), 2.80 (t, 2H, -CH$_2$-CH$_2$-OH), 2.87 (m, 2H, CH$_2$-N), 3.53 (m, 2H, -CH$_2$-CH$_2$-OH), 3.85 (m, 1H, CH-N), 4.98 (br, 1H for one isomer), 5.08 (br, 1H for the other), 7.40 (d, 2H), 7.82 (d, 2H), 9.08 (br 1H for one isomer, NH$_2$$^+$), 9.46 (br, 1H for the other, NH$_2$$^+$), 10.85 (s, 1H, NH).

N^1-(4-Chlorophenyl)-N^2-(1-(5-(2-hydroxyethyl)-4-methylthiazol-2-yl)-2-(methylamino)ethyl)oxalamide·2HCl (16). White solid. Yield: 41%. LC−MS (APCI$^+$) m/z: calcd for C$_{17}$H$_{21}$ClN$_4$O$_3$S, 396.10; found, 397.08 (M + H$^+$). HPLC: 94.2%. ^{1}H NMR (DMSO-d_6, 50 °C, 400 MHz) δ_H, 2.27 (s, 3H, -CH$_3$), 2.59 (br, 3H, NH-CH$_3$), 2.82 (m, 2H, -CH$_2$-CH$_2$-OH), 3.55 (m, 3H, -NCH$_3$), 3.60 (m, 2H, -CH$_2$-OH), 5.30 (m, 2H), 5.55 (m, 1H, CH-HetAr), 7.41 (d, 2H, ArH), 7.82 (d, 2H, ArH), 9.05 (br 1H, NH), 9.28 (br 1H, NH), 9.75 (br d, 1H, NH), 10.85 (s, 1H, NH).

N^1-(4-Chlorophenyl)-N^2-(1-ethyl-1H-pyrazol-4-yl)oxalamide (17). White solid. Yield: 35%. Mp: 232−233. LC−MS (APCI$^+$) m/z: calcd for C$_{13}$H$_{13}$ClN$_4$O$_2$: 292.07; found, 293.04 (M + H$^+$). HPLC: 98.8%. ^{1}H NMR (DMSO-d_6, 400 MHz) δ_H, 1.38 (t, 3H, -CH$_3$), 4.11 (q, 2H, -CH$_2$-), 7.41 (d, 2H, Ar-H), 7.70 (s, 1H, HetAr-H), 7.86 (d, 2H, Ar-H), 8.10 (s, 1H, HetAr-H), 10.75 (s, 1H, NH), 11.10 (s, 1H, NH).

(2S,4R,5S)-Methyl 4-(2-(4-Chlorophenylamino)-2-oxoacetamido)-5-phenylpyrrolidine-2-carboxylate (18). White solid. Yield: 39%. LC−MS (APCI$^+$) m/z: calcd for C$_{20}$H$_{20}$ClN$_3$O$_4$: 401.11; found, 402.14 (M + H$^+$). HPLC: 95%. ^{1}H NMR (DMSO-d_6, 50 °C, 400 MHz) δ_H, 2.18 (m, 2H, -CH$_2$-), 3.30 (br, 1H, -NH-), 3.69 (s, 3H, O-CH$_3$), 4.05 (m, 1H, -N-CH-Ph), 4.17 (m, 1H, -CH-), 4.27 (m, 1H, -CH-), 7.20 (t, 1H, Ar-H), 7.28 (t, 2H, Ar-H meta), 7.38 (d, 2H, Ar-H), 7.44 (d, 2H, Ar-H), 7.81 (d, 2H, Ar-H), 9.12 (br 1H, NH), 10.58 (s, 1H, Ar-NH).

N^1-(4-Chlorophenyl)-N^2-((1S,2R)-1-morpholino-1-phenylpropan-2-yl)oxalamide (19). White solid. Yield: 30%. LC−MS (APCI$^+$) m/z: calcd for C$_{21}$H$_{24}$ClN$_3$O$_3$: 401.15; found, 402.28 (M + H$^+$). HPLC: 95%. ^{1}H NMR (CDCl$_3$, 45 °C, 400 MHz) δ_H 1.10 (d, 3H, -CH$_3$), 2.45 (br, 2H, -N-CH$_2$-), 2.56 (br, 2H, -N-CH$_2$-), 3.31 (d, 1H, Ph-CH-N), 3.79 (m br, 4H, -O-CH$_2$-), 4.65 (m, 1H, N-CH-CH$_3$), 7.28−7.45 (m, 5H, Ar-H), 7.52 (br d, 2H, Ar-H), 7.57 (br d, 2H, Ar-H).

N^1-((5-(Hydroxymethyl)-4-methylthiazol-2-yl)(piperidin-2-yl)methyl)-N^2-(4-(trifluoromethyl)phenyl)oxalamide·2HCl (20). White solid. Yield: 56% (diastereoisomeric mixture, 1:20). LC−MS (APCI$^+$) m/z: calcd for C$_{20}$H$_{23}$F$_3$N$_4$O$_3$S, 456.14; found, 457.90 (M + H$^+$). HPLC: 97.7%. ^{1}H NMR (DMSO-d_6, 50 °C, 400 MHz) δ_H, 1.30−1.76 (m, 6H), 2.27 (s, 3H, -CH$_3$), 2.62 (br, 1H, CH), 3.30, (br d, 1H), 3.82 (br, 1H), 4.56 (s, 2H, -CH$_2$-O), 5.40 (t, 1H for one isomer), 5.51 (t, 1H for the other), 7.65 (d, 2H), 8.20 (d, 2H), 8.61−9.50 (m, 2H, NH$_2$$^+$), 9.65 (br d, 1H, CONH), 11.00 (s, 1H for one isomer, CONH), 11.08 (s, 1H for the other, CONH).

N^1-(2,4-Difluorophenyl)-N^2-((5-(hydroxymethyl)-4-methylthiazol-2-yl)(piperidin-2-yl)methyl)oxalamide·HCl (21). White solid. Yield: 58% (diastereoisomeric mixture, 1:5). LC−MS (APCI$^+$) m/z: calcd for C$_{19}$H$_{22}$F$_2$N$_4$O$_3$S, 424.14; found, 425.86 (M + H$^+$). HPLC: 95.6%. ^{1}H NMR (DMSO-d_6, 50 °C, 400 MHz) δ_H, 1.30−1.80 (m, 6H), 2.27 (s, 3H, -CH$_3$), 2.80−4.00 (m, 3H + H$_2$O signal), 4.56 (s, 2H, -CH$_2$-O), 5.35 (t, 1H for one isomer), 5.41 (t, 1H for the other), 7.11 (t, 1H), 7.34 (t, 3H), 7.61 (m, 3H), 8.38 (br 1H, NH$_2$$^+$), 8.70 (br d, 1H, NH$_2$$^+$), 9.51 (d, 1H for one isomer, NH), 9.70 (d, 1H for the other, NH), 10.25 (s, 1H for one isomer, Ar-CONH), 10.30 (s, 1H for the other, Ar-CONH).

N^1-(3,4-Difluorophenyl)-N^2-((5-(hydroxymethyl)-4-methylthiazol-2-yl)(piperidin-2-yl)methyl)oxalamide·HCl (22). White solid. Yield: 45% (diastereoisomeric mixture, 3:2). LC−MS (APCI$^+$) m/z: calcd for C$_{19}$H$_{22}$F$_2$N$_4$O$_3$S, 424.14; found, 425.90 (M + H$^+$). HPLC: 98.3%. ^{1}H NMR (DMSO-d_6, 50 °C, 400 MHz) δ_H, 1.30−1.80 (m, 6H), 2.27 (s, 3H -CH$_3$), 2.82 (br, 1H), 3.30, (br, 1H), 3.82 (m, 1H), 4.56 (s, 2H, -CH$_2$-O), 5.40 (t, 1H for one isomer), 5.55 (t, 1H for the other), 7.40 (m, 1H), 7.67 (d, 1H) 7.91 (m, 1H), 8.60 (br, 1H for one isomer, NH$_2$$^+$), 8.90 (br, 1H for the other, NH$_2$$^+$), 9.20 (br, 1H for one isomer, NH$_2$$^+$), 9.35 (br, 1H for the other, NH$_2$$^+$), 9.68 (br d + d, 1H, CONH), 10.80 (s, 1H, CONH-Ar), 11.00 (s, 1H, CONH-Ar).

N^1-(4-Acetylphenyl)-N^2-((5-(hydroxymethyl)-4-methylthiazol-2-yl)(piperidin-2-yl)methyl)oxalamide·HCl (23). White solid. Yield: 42% (diastereoisomeric mixture, 3:2). LC−MS (APCI$^+$) m/z: calcd for C$_{21}$H$_{26}$N$_4$O$_4$S, 430.17; found, 431.19 (M + H$^+$). HPLC: 96.5%. ^{1}H NMR (DMSO-d_6, 50 °C, 400 MHz) δ_H, 1.30−1.80 (m, 6H), 2.27 (s, 3H, -CH$_3$), 2.52 (s, 3H, -CH$_3$), 2.82 (br, 1H), 3.30, (br, 1H), 3.82 (m, 1H), 4.56 (s, 2H, -CH$_2$-O), 5.40 (t, 1H for one isomer), 5.55 (t, 1H for the other), 7.90 (s, 4H, ArH), 8.60 (br, 1H for one isomer, NH$_2$$^+$), 8.95 (br, 1H for the other, NH$_2$$^+$), 9.10 (br, 1H for one isomer, NH$_2$$^+$), 9.25 (br, 1H for the other, NH$_2$$^+$), 9.65 (d, 1H for one isomer, CONH), 9.71 (d, 1H for the other, CONH), 10.80 (s, 1H, CONH-Ar), 11.00 (s, 1H, CONH-Ar).

N^1-(3-Chloro-4-fluorophenyl)-N^2-((5-(hydroxymethyl)-4-methylthiazol-2-yl)(piperidin-2-yl)methyl)oxalamide·2HCl (24). White solid. Yield: 33% (diastereoisomeric mixture, 1:1). LC−MS (APCI$^+$) m/z: calcd for C$_{19}$H$_{22}$ClFN$_4$O$_3$S, 440.11; found, 441.13 (M + H$^+$). HPLC: 92.7%. ^{1}H NMR (DMSO-d_6, 50 °C, 400 MHz) δ_H, 1.30−1.80 (m, 6H), 2.27 (s, 3H, -CH$_3$), 2.82 (br, 1H), 3.30, (br, 1H), 3.82 (br, 1H), 4.56 (s, 2H, -CH$_2$-O), 5.40 (t, 1H for one isomer), 5.55 (t, 1H for the other), 7.40 (t, 1H, ArH), 7.82 (m, 1H, ArH), 8.08 (m, 1H ArH), 8.60 (br, 1H for one isomer, NH$_2$$^+$), 8.95 (br, 1H for the other, NH$_2$$^+$), 9.19 (br, 1H for one isomer, NH$_2$$^+$), 9.40 (br, 1H for the other, NH$_2$$^+$), 9.68 (d + d, 1H, CONH), 10.80 (s, 1H, CONH-Ar), 11.00 (s, 1H, CONH-Ar).

N^1-(4-Fluorophenyl)-N^2-((5-(hydroxymethyl)-4-methylthiazol-2-yl)(piperidin-2-yl)methyl)oxalamide·HCl (25). White solid. Yield: 50% (diastereoisomeric mixture, 1:1). LC−MS (APCI$^+$) m/z: calcd for C$_{19}$H$_{23}$FN$_4$O$_3$S, 406.15; found, 407.16 (M + H$^+$). HPLC: 94.7%. ^{1}H NMR (DMSO-d_6, 50 °C, 400 MHz) δ_H, 1.30−1.80 (m, 6H), 2.27 (s, 3H, -CH$_3$), 2.80−3.00 (br, 1H), 3.30 (br, 1H), 3.82 (m, 1H), 4.51 (s, 2H, -CH$_2$-O), 5.40 (t, 1H for one isomer), 5.51 (t, 1H for

the other), 7.12 (m, 2H, Ar$\underline{H}$), 7.75 (m, 2H, Ar$\underline{H}$), 8.60 (br, 1H for one isomer, N$\underline{H}_2^+$), 8.95 (br, 1H for the other, N$\underline{H}_2^+$), 9.19 (br, 1H for one isomer, N$\underline{H}_2^+$), 9.40 (br, 1H for the other, N$\underline{H}_2^+$), 9.65 (d + d, 1H, CON$\underline{H}$), 10.70 (s, 1H for one isomer, CON$\underline{H}$-Ar), 10.75 (s, 1H for the other, CON$\underline{H}$-Ar).

N^1-(2-Fluoro-4-methylphenyl)-N^2-((5-(hydroxymethyl)-4-methylthiazol-2-yl)(piperidin-2-yl)methyl)oxalamide·HCl (26). White solid. Yield: 39% (diastereoisomeric mixture, 1:9). LC−MS (APCI$^+$) m/z: calcd for $C_{20}H_{25}FN_4O_3S$:420.16; found, 421.19 (M + H$^+$). HPLC: 95.1%. ^{1}H NMR (DMSO-d_6, 50 °C, 400 MHz) δ_H, 1.30−1.80 (m, 6H), 2.27 (s, 3H, -HetAr-C$\underline{H}_3$), 2.31 (s, 3H, Ar-C$\underline{H}_3$), 2.75−3.00 (br, 1H), 3.30 (br, 1H), 3.82 (m, 1H), 4.51(s, 2H, -C$\underline{H}_2$-O), 5.40 (t, 1H for one isomer), 5.51 (t, 1H for the other), 7.02 (d, 1H, Ar$\underline{H}$), 7.10 (d, 1H, Ar$\underline{H}$), 7.50 (t, 1H, Ar$\underline{H}$), 8.51 (br, 1H for one isomer, N$\underline{H}_2^+$), 8.61 (br, 1H for the other, N$\underline{H}_2^+$), 9.10 (br d, 1H for one isomer, N$\underline{H}_2^+$), 9.25 (br, 1H for the other, N$\underline{H}_2^+$), 9.60 (d, 1H for one isomer, CON$\underline{H}$), 9.67 (d, 1H for the other, CON$\underline{H}$), 10.10 (s, 1H for one isomer, CON$\underline{H}$-Ar), 10.20 (s, 1H for the other, CON$\underline{H}$-Ar).

N^1-(3-Fluoro-4-methylphenyl)-N^2-((5-(hydroxymethyl)-4-methylthiazol-2-yl)(piperidin-2-yl)methyl)oxalamide·HCl (28). White solid. Yield: 34% (diastereoisomeric mixture, 2:3). LC−MS (APCI$^+$) m/z: calcd for $C_{20}H_{25}FN_4O_3S$, 420.16; found, 421.19 (M + H$^+$). HPLC: 95.8%. ^{1}H NMR (DMSO-d_6, 50 °C, 400 MHz) δ_H, 1.30−1.80 (m, 6H), 2.26 (s, 3H, -C$\underline{H}_3$), 2.80 (m, 1H), 3.30, (br, 1H), 3.80 (m, 1H,), 4.56 (s, 2H, C$\underline{H}_2$-OH), 5.40 (t, 1H for one isomer), 5.51 (t, 1H for the other), 7.24 (m, 1H, Ar$\underline{H}$), 7.55 (d, 1H, Ar$\underline{H}$), 7.66 (d, 1H, Ar$\underline{H}$), 8.51 (br, 1H for one isomer, N$\underline{H}_2^+$), 8.65 (br, 1H for the other, N$\underline{H}_2^+$), 9.11 (br, 1H for one isomer, N$\underline{H}_2^+$), 9.24 (br, 1H for the other, N$\underline{H}_2^+$), 9.61 (d, 1H for one isomer, CON$\underline{H}$), 9.68 (d, 1H for the other, CON$\underline{H}$), 10.75 (s, 1H for one isomer, CON$\underline{H}$-Ar), 10.82 (s, 1H for the other, CON$\underline{H}$-Ar).

N^1-Cycloheptyl-N^2-((5-(hydroxymethyl)-4-methylthiazol-2-yl)(piperidin-2-yl)methyl)oxalamide·HCl (29). White solid. Yield: 28% (diastereoisomeric mixture, 2:3). LC−MS (APCI$^+$) m/z: calcd for $C_{20}H_{32}N_4O_3S$, 408.22; found, 409.57 (M + H$^+$). HPLC: 97.5%. ^{1}H NMR (DMSO-d_6, 50 °C, 400 MHz) δ_H, 1.30−1.80 (m, 18H), 2.26 (s, 3H, -C$\underline{H}_3$), 2.75−3.00 (m, 1H), 3.27, (m, 1H), 3.40, (m, 1H), 3.76 (m, 2H), 4.56 (s, 2H, C$\underline{H}_2$-OH), 5.33 (t, 1H for one isomer), 5.50 (t, 1H for the other), 8.30−8,55 (br m, 1H, N$\underline{H}$), 8.53 (br, 1H for one isomer, N$\underline{H}$), 8.77 (br, 1H for the other, N$\underline{H}$), 9.11 (br, 1H for one isomer, N$\underline{H}$), 9.25 (br, 1H for the other, N$\underline{H}$), 9.40 (br, 1H, CO-N$\underline{H}$).

N^1-(4-Chlorophenyl)-N^2-((5-(2-hydroxyethyl)-4-methylthiazol-2-yl)(piperidin-2-yl)methyl)oxalamide·HCOOH (30). White solid. Yield: 55% (diastereoisomeric mixture, 1:1). LC−MS (APCI$^+$) m/z: calcd for $C_{20}H_{25}ClN_4O_3S$:436.13; found, 437.30 (M + H$^+$). HPLC: >95.0%. ^{1}H NMR (DMSO-d_6, 50 °C, 400 MHz) δ_H, 1.10−1.80 (m, 6H), 2.26 (s, 3H, -C$\underline{H}_3$), 2.75−3.00 (m, 3H), 3.00−3.80 (12H + NH + H$_2$O signal), 5.00 (br, 1H for one isomer), 5.10 (br, 1H for the other), 7.41 (d, 2H), 7.82 (d, 2H), 9.10 (br 1H for one isomer, N$\underline{H}_2^+$), 9.38 (br, 1H for the other, N$\underline{H}_2^+$), 10.85 (s, 1H, N$\underline{H}$).

N^1-((5-(2-Hydroxyethyl)-4-methylthiazol-2-yl)(piperidin-2-yl)methyl)-N^2-(4-(trifluoromethyl)phenyl)oxalamide·2HCl (31). White solid. Yield: 39% (diastereoisomeric mixture, 1:1). LC−MS (APCI$^+$) m/z: calcd for $C_{21}H_{25}F_3N_4O_3S$, 470.16; found, 471.21 (M + H$^+$). HPLC: 95.5%. ^{1}H NMR (DMSO-d_6, 50 °C, 400 MHz) δ_H, 1.30−1.80 (m, 6H), 2.25 (s, 3H, -C$\underline{H}_3$) 2.75−3.00 (m, 3H), 3.30, (br, 1H), 3,55 (m, 2H, -C$\underline{H}_2$-C$\underline{H}_2$-OH), 3.80 (br, 1H), 5.38 (t, 1H for one isomer), 5.55 (t, 1H for the other), 7.77 (d, 2H, Ar$\underline{H}$), 8.02 (d, 2H, Ar$\underline{H}$), 8.60 (br, 1H for one isomer, N$\underline{H}_2^+$), 8.91 (br, 1H for the other, N$\underline{H}_2^+$), 9.12 (br, 1H for one isomer, N$\underline{H}_2^+$), 9.26 (br, 1H for the other, N$\underline{H}_2^+$), 9.63 (d, 1H for one isomer, CON$\underline{H}$), 9.70 (d, 1H for the other, CON$\underline{H}$), 10.98 (s, 1H for one isomer, CON$\underline{H}$-Ar), 11.20 (s, 1H for the other, CON$\underline{H}$-Ar).

N^1-(2,4-Difluorophenyl)-N^2-((5-(2-hydroxyethyl)-4-methylthiazol-2-yl)(piperidin-2-yl)methyl)oxalamide·HCl (32). White solid. Yield: 43% (diastereoisomeric mixture, 1:1). LC−MS (APCI$^+$) m/z: calcd for $C_{20}H_{24}F_2N_4O_3S$, 438.15; found 438.50 (M + H$^+$). HPLC: 97.5%. ^{1}H NMR (DMSO-d_6, 50 °C, 400 MHz) δ_H, 1.30−1.80 (m, 6H), 2.25 (s, 3H, -C$\underline{H}_3$), 2.75−3.00 (m, 3H), 3.30, (br, 1H), 3.55 (m, 2H, -C$\underline{H}_2$-C$\underline{H}_2$-OH), 3.80 (br, 1H), 5.39 (t, 1H for one isomer),

5.50 (t, 1H for the other), 7.07 (m, 1H, Ar$\underline{H}$), 7.28 (m, 1H, Ar$\underline{H}$), 7.60 (m, 1H, Ar$\underline{H}$), 8.50 (br, 1H for one isomer, N$\underline{H}_2^+$), 8.74 (br, 1H for the other, N$\underline{H}_2^+$), 9.09 (br, 1H for one isomer, N$\underline{H}_2^+$), 9.21 (br, 1H for the other, N$\underline{H}_2^+$), 9.57 (d, 1H for one isomer, CON$\underline{H}$), 9.70 (d, 1H for the other, CON$\underline{H}$), 11.01 (s, 1H for one isomer, CON$\underline{H}$-Ar), 11.32 (s, 1H for the other, CON$\underline{H}$-Ar).

N^1-(3,4-Difluorophenyl)-N^2-((5-(2-hydroxyethyl)-4-methylthiazol-2-yl)(piperidin-2-yl)methyl)oxalamide·2HCl (33). White solid. Yield: 32% (diastereoisomeric mixture, 1:1). LC−MS (APCI$^+$) m/z: calcd for $C_{20}H_{24}F_2N_4O_3S$, 438.15; found, 439.19 (M + H$^+$). HPLC: 97.9%. ^{1}H NMR (DMSO-d_6, 50 °C, 400 MHz) δ_H, 11.30−1.80 (m, 6H), 2.25 (s, 3H, -C$\underline{H}_3$), 2.75−3.00 (m, 3H), 3.30, (br, 1H), 3,55 (m, 2H, -C$\underline{H}_2$-C$\underline{H}_2$-OH), 3.80 (br, 1H), 5.36 (t, 1H for one isomer), 5.50 (t, 1H for the other), 7.40 (m, 1H, Ar$\underline{H}$), 7.65 (m, 1H, Ar$\underline{H}$), 7.91 (m, 1H, Ar$\underline{H}$), 8.56 (br, 1H for one isomer, N$\underline{H}_2^+$), 8.90 (br, 1H for the other, N$\underline{H}_2^+$), 9.11 (br d, 1H for one isomer, N$\underline{H}_2^+$), 9.29 (br, 1H for the other, N$\underline{H}_2^+$), 9.61 (d, 1H for one isomer, CON$\underline{H}$), 9.69 (d, 1H for the other, CON$\underline{H}$), 10.85 (s, 1H for one isomer, CON$\underline{H}$-Ar), 11.00 (s, 1H for the other, CON$\underline{H}$-Ar).

N^1-(4-Acetylphenyl)-N^2-((5-(2-hydroxyethyl)-4-methylthiazol-2-yl)(piperidin-2-yl)methyl)oxalamide·2HCl (34). White solid. Yield: 44% (diastereoisomeric mixture, 1:1). LC−MS (APCI$^+$) m/z: calcd for $C_{22}H_{28}N_4O_4S$, 444.18; found, 445.20 (M + H$^+$). HPLC: 96.6%. ^{1}H NMR (DMSO-d_6, 50 °C, 400 MHz) δ_H, 1.30−1.80 (m, 6H), 2.25 (s, 3H, -C$\underline{H}_3$), 2.52 (s, 3H, CO-C$\underline{H}_3$), 2.75−3.00 (br, 3H), 3.30, (br, 1H), 3.55 (m, 2H, -C$\underline{H}_2$-C$\underline{H}_2$-OH), 3.80 (br, 1H), 5.36 (t, 1H for one isomer), 5.50 (t, 1H for the other), 7.86 (s, 4H, Ar$\underline{H}$), 8.56 (br, 1H for one isomer, N$\underline{H}_2^+$), 8.90 (br, 1H for the other, N$\underline{H}_2^+$), 9.10 (br, 1H for one isomer, N$\underline{H}_2^+$), 9.25 (br, 1H for the other, N$\underline{H}_2^+$), 9.61 (d, 1H for one isomer, CON$\underline{H}$), 9.69 (d, 1H for the other, CON$\underline{H}$), 10.86 (s, 1H for one isomer, CON$\underline{H}$-Ar), 11.00 (s, 1H for the other, CON$\underline{H}$-Ar).

N^1-(3-Chloro-4-fluorophenyl)-N^2-((5-(2-hydroxyethyl)-4-methylthiazol-2-yl)(piperidin-2-yl)methyl)oxalamide·2HCl (35). White solid. Yield: 35% (diastereoisomeric mixture, 1:1). LC−MS (APCI$^+$) m/z: calcd for $C_{20}H_{24}ClFN_4O_3S$, 454.12; found, 455.14 (M + H$^+$). HPLC: 97.0%. ^{1}H NMR (DMSO-d_6, 50 °C, 400 MHz) δ_H, 1.30−1.80 (m, 6H), 2.25 (s, 3H, -C$\underline{H}_3$), 2.75−3.00 (m, 3H), 3.30, (br, 1H), 3.55 (m, 2H), 3.80 (br, 1H), 5.39 (t, 1H for one isomer), 5.51 (t, 1H for the other), 7.40 (t, 1H, Ar$\underline{H}$), 7.80 (m, 1H, Ar$\underline{H}$), 8.15 (m, 1H, Ar$\underline{H}$), 8.58 (br, 1H for one isomer, N$\underline{H}_2^+$), 8.90 (br, 1H for the other, N$\underline{H}_2^+$), 9.15 (br, 1H for one isomer, N$\underline{H}_2^+$), 9.30 (br, 1H for the other, N$\underline{H}_2^+$), 9.61 (d, 1H for one isomer, CON$\underline{H}$), 9.69 (d, 1H for the other, CON$\underline{H}$), 10.86 (s, 1H for one isomer, CON$\underline{H}$-Ar), 11.00 (s, 1H for the other, CON$\underline{H}$-Ar).

N^1-(4-Fluorophenyl)-N^2-((5-(2-hydroxyethyl)-4-methylthiazol-2-yl)(piperidin-2-yl)methyl)oxalamide·HCl (36). White solid. Yield: 47% (diastereoisomeric mixture, 1:1.2). LC−MS (APCI$^+$) m/z: calcd for $C_{20}H_{25}FN_4O_3S$, 420.16; found, 421.18 (M + H$^+$). HPLC: 95.3%. ^{1}H NMR (DMSO-d_6, 50 °C, 400 MHz) δ_H, 1.30−1.80 (m, 6H), 2.26 (s, 3H, -C$\underline{H}_3$), 2.75−3.00 (m, 3H), 3.30 (br, 1H), 3.55 (m, 2H), 3.80 (br, 1H), 5.39 (t, 1H for one isomer), 5.50 (t, 1H for the other), 7.17 (m, 2H, Ar$\underline{H}$), 7.82 (m, 2H, Ar$\underline{H}$), 8.51 (br, 1H for one isomer, N$\underline{H}_2^+$), 8.90 (br, 1H for the other, N$\underline{H}_2^+$), 9.12 (br, 1H for one isomer, N$\underline{H}_2^+$), 9.28 (br, 1H for the other, N$\underline{H}_2^+$), 9.51 (d, 1H for one isomer, CON$\underline{H}$), 9.60 (d, 1H for the other, CON$\underline{H}$), 10.70 (s, 1H for one isomer, CON$\underline{H}$-Ar), 10.76 (s, 1H for the other, CON$\underline{H}$-Ar).

N^1-(2-Fluoro-4-methylphenyl)-N^2-((5-(2-hydroxyethyl)-4-methylthiazol-2-yl)(piperidin-2-yl)methyl)oxalamide·2HCl (37). White solid. Yield: 65% (diastereoisomeric mixture, 1:1). LC−MS (APCI$^+$) m/z: calcd for $C_{21}H_{27}FN_4O_3S$, 434.18; found, 435.21 (M + H$^+$). HPLC: 93.4%. ^{1}H NMR (DMSO-d_6, 50 °C, 400 MHz) δ_H, 1.30−1.80 (m, 6H), 2.26 (s, 3H, -C$\underline{H}_3$), 2.75−3.00 (m, 3H), 3.30, (br, 1H), 3.60 (m, 2H), 3.80 (br, 1H), 5.35 (t, 1H for one isomer), 5.50 (t, 1H for the other), 7.01 (d, 1H, Ar$\underline{H}$), 7.10 (d, 1H, Ar$\underline{H}$), 7.51 (m, 1H, Ar$\underline{H}$), 8.51 (br, 1H for one isomer, N$\underline{H}_2^+$), 8.65 (br, 1H for the other, N$\underline{H}_2^+$), 9.11 (br, 1H for one isomer, N$\underline{H}_2^+$), 9.24 (br, 1H for the other, N$\underline{H}_2^+$), 9.53 (d, 1H for one isomer, CON$\underline{H}$), 9.70 (d, 1H for the other, CON$\underline{H}$), 10.15 (s, 1H for one isomer, CON$\underline{H}$-Ar), 10.24 (s, 1H for the other, CON$\underline{H}$-Ar).

N^1-(3-Fluoro-4-methylphenyl)-N^2-((5-(2-hydroxyethyl)-4-methylthiazol-2-yl)(piperidin-2-yl)methyl)oxalamide·HCl (38). White solid. Yield: 47% (diastereoisomeric mixture, 1:1). LC−MS (APCI$^+$) m/z: calcd for $C_{21}H_{27}FN_4O_3S$, 434.18; found, 435.24 (M + H$^+$). HPLC: 96.1%. ^{1}H NMR (DMSO-d_6, 50 °C, 400 MHz) δ_H, 1.30−1.80 (m, 6H), 2.20 (s, 3H, Ar-C$\underline{H}_3$), 2.26 (s, 3H, HetAr-C$\underline{H}_3$), 2.75−3.00 (m, 3H), 3.30 (br, 1H), 3.55 (m, 2H, -CH$_2$-C$\underline{H}_2$-OH), 3.80 (s, 1H), 5.39 (t, 1H for one isomer), 5.57 (t, 1H for the other), 7.24 (t, 1H, Ar$\underline{H}$), 7.55 (d, 1H, Ar$\underline{H}$), 7.70 (d, 1H, Ar$\underline{H}$), 8.55 (br, 1H for one isomer, N$\underline{H}_2^+$), 8.91 (br, 1H for the other, N$\underline{H}_2^+$), 9.12 (br d, 1H for one isomer, N$\underline{H}_2^+$), 9.26 (br, 1H for the other, N$\underline{H}_2^+$), 9.58 (d, 1H for one isomer, CON$\underline{H}$), 9.65 (d, 1H for the other, CON$\underline{H}$), 10.75 (s, 1H for one isomer, CON$\underline{H}$-Ar), 10.80 (s, 1H for the other, CON$\underline{H}$-Ar).

N^1-(4-Chloro-3-fluorophenyl)-N^2-((5-(2-hydroxyethyl)-4-methylthiazol-2-yl)(piperidin-2-yl)methyl)oxalamide·HCl (39). White solid. Yield: 50% (diastereoisomeric mixture, 4:5). LC−MS (APCI$^+$) m/z: calcd for $C_{20}H_{24}ClFN_4O_3S$, 454.12; found, 455.18 (M + H$^+$). HPLC: 96.2%. ^{1}H NMR (DMSO-d_6, 50 °C, 400 MHz) δ_H, 1.30−1.80 (m, 6H), 2.26 (s, 3H, -C$\underline{H}_3$), 2.75−3.00 (m, 3H), 3.30 (br, 1H), 3.60 (m, 2H, -CH$_2$-C$\underline{H}_2$-OH), 3.80 (m, 1H,), 5.35 (t, 1H for one isomer), 5.50 (t, 1H for the other), 7.55 (t, 1H, Ar$\underline{H}$), 7.65 (d, 1H, Ar$\underline{H}$), 7.90 (d, 1H, Ar$\underline{H}$), 8.59 (br, 1H for one isomer, N$\underline{H}_2^+$), 8.90 (br, 1H for the other, N$\underline{H}_2^+$), 9.11 (br, 1H for one isomer, N$\underline{H}_2^+$), 9.24 (br, 1H for the other, N$\underline{H}_2^+$), 9.60 (d, 1H for one isomer, CON$\underline{H}$), 9.68 (d, 1H for the other, CON$\underline{H}$), 10.92 (s, 1H for one isomer, CON$\underline{H}$-Ar), 11.09 (s, 1H for the other, CON$\underline{H}$-Ar).

N^1-Cycloheptyl-N^2-((5-(2-hydroxyethyl)-4-methylthiazol-2-yl)(piperidin-2-yl)methyl)oxalamide·HCl (40). Yellow oil. Yield: 57% (diastereoisomeric mixture, 1:1). LC−MS (APCI$^+$) m/z: calcd for $C_{21}H_{34}N_4O_3S$, 422.24; found, 423.60 (M + H$^+$). HPLC: 98.5%. ^{1}H NMR (DMSO-d_6, 50 °C, 400 MHz) δ_H, 1.30−1.80 (m, 18H), 2.26 (s, 3H, -C$\underline{H}_3$), 2.75−3.00 (m, 3H), 3.30 (br, 1H), 3.40 (m, 1H), 3.58 (m, 2H, -CH$_2$-C$\underline{H}_2$-OH), 3.80 (m, 1H), 5.35 (t, 1H for one isomer), 5.50 (t, 1H for the other), 8.30−8.55 (br m, 1Hσ, N$\underline{H}$), 8.53 (br, 1H for one isomer, N$\underline{H}$), 8.77 (br, 1H for the other, N$\underline{H}$), 9.11 (br, 1H for one isomer, N$\underline{H}$), 9.25 (br, 1H for the other, N$\underline{H}$), 9.40 (br, 1H, CO-N$\underline{H}$).

Measurement of Antiviral Activity. *Pseudoviruses Preparation.* To prepare the X4-tropic pseudovirus NL4-3-HXB2-Luc, 5×10^6 293T cells were seeded in a T75 flask and transfected 24 h later in 20 mL of medium with a mixture of 10 μg of pNL4-3.Luc.R-E- DNA and 10 μg of env expression vector pHXB2-env (X4) DNA using FuGENE 6 (Roche). Pseudovirus-containing supernatant was collected 2 days after transfection and stored in aliquots at −80 °C. Pseudovirus was titered by infecting the TZM-bl cells to calculate the 50% tissue culture infectious dose (TCID$_{50}$). TZM-bl cells were plated in 96-well plates at 10^4 cells/well 24 h before infection. On the day of the infection 100 μL of serial 2-fold dilutions of pseudovirus were added to the cells. After 3 days of incubation the cells were washed 2 times with PBS and lysed with 50 μL of cell culture lysis reagent (Promega). An amount of 20 μL of lysates was transferred to a white 96-well plate (Costar) and mixed with 100 μL of luciferase assay reagent (luciferase assay system, Promega). The luciferase activity was immediately measured with a Tecan infinite M1000 reader (Tecan). Wells producing relative luminescence units (RLU) 4 times the background were scored as positive, and the TCID$_{50}$ was calculated by the Spearman−Karber statistical method.

Single-Cycle Neutralization Assay. The inhibitory activity of small molecules was tested on NL4-3-HXB2-Luc pseudotyped virus expressing Env of the HIV-1$_{HXB2}$ (X4). Briefly, 100 μL of TZM-bl cells at 1×10^5 cells/mL was added to the wells of a 96-well tissue culture plate and cultured at 37 °C overnight. Then 50 μL of a test compound at graded concentrations was mixed with 50 μL of the NL4-3-HXB2-Luc virus at about 100 TCID$_{50}$. After incubation at 37 °C for 30 min, the mixtures were added to the cells and incubated at 37 °C for 3 days. The cells were then harvested and lysed for measuring luciferase activity as described above.

Multicycle Neutralization Assay. The inhibitory activity of small molecules on infection by laboratory-adapted HIV-1 IIIB strain was

determined as previously described.[26] In brief, 1×10^4 MT-2 cells were infected with HIV-1 at 100 TCID$_{50}$ (50% tissue culture infective dose) (0.01 MOI) in 200 μL of medium in the presence or absence of small molecules at graded concentrations and incubated overnight. The culture supernatants were then removed and replaced with fresh medium. On the fourth day postinfection, an amount of 100 μL of culture supernatants was collected from each well, mixed with an equal volume of 5% Triton X-100, and tested for p24 antigen by sandwich-ELISA. The percent inhibition of p24 production and IC$_{50}$ values were calculated by the GraphPad Prism software (GraphPad Software Inc.).

Determination of Cytotoxicity. *In TZM-bl Cells.* The cytotoxicity of small molecules in TZM-bl cells was measured by a colorimetric method using XTT (sodium 3′-(1-(phenylamino)carbonyl)-3,4-tetrazolium-bis(4-methoxy-6-nitro)bezenesulfonic acid hydrate), a light yellowish tetrazolium dye, as previously described.[27] Briefly, 100 μL of a compound at graded concentrations was added to equal volume of cells (10^5/mL) in wells of 96-well plates followed by incubation at 37 °C for 3 days and addition of XTT (PolySciences, Inc., Warrington, PA). The soluble intracellular formazan was quantitated colorimetrically at 450 nm 4 h later. The percent of cytotoxicity and the CC$_{50}$ (the concentration for 50% cytotoxicity) values were calculated by the GraphPad Prism software (GraphPad Software Inc.).

In MT-2 Cells. Cytotoxicity of small molecules in MT-2 cells was measured as previously described.[26] Briefly, 100 μL of a small molecule at graded concentrations was added to an equal volume of MT-2 cells (10^5 cells/mL) in 96-well plates followed by incubation at 37 °C for 4 days. After addition of XTT, the soluble intracellular formazan was quantitated colorimetrically and the percent of cytotoxicity and the CC$_{50}$ values were calculated as above.

ASSOCIATED CONTENT

Ⓢ Supporting Information

Synthesis procedures (Scheme S1) of succinamide series compounds (**41−51**), listing of their structures and antiviral activity (Table S1), and listing of the 50 top GLIDE XP-scored poses (Figure S1). This material is available free of charge via the Internet at http://pubs.acs.org.

AUTHOR INFORMATION

Corresponding Author

*Phone: (212) 570-3373. E-mail: adebnath@nybloodcenter.org.

Notes

The authors declare no competing financial interest.

ABBREVIATIONS USED

SAR, structure−activity relationship; LC−MS, liquid chromatography−mass spectrometry; NMR, nuclear magnetic resonance; DCM, dichloromethane; TBTU, $N,N,N′,N′$-tetramethyl-O-(benzotriazol-1-yl)uranium tetrafluoroborate

REFERENCES

(1) Wyatt, R.; Sodroski, J. G. The HIV-1 envelope glycoproteins: fusogens, antigens, and immunogens. *Science* **1998**, *280*, 1884−1888.
(2) Doms, R. W. Chemokine receptors and HIV entry. *AIDS* **2001**, *15* (Suppl. 1), S34−S35.
(3) Duffalo, M. L.; James, C. W. Enfuvirtide: a novel agent for the treatment of HIV-1 infection. *Ann. Pharmacother.* **2003**, *37*, 1448−1456.

(4) Hardy, H.; Skolnik, P. R. Enfuvirtide, a new fusion inhibitor for therapy of human immunodeficiency virus infection. *Pharmacotherapy* **2004**, *24*, 198−211.

(5) Meanwell, N. A.; Kadow, J. F. Maraviroc, a chemokine CCR5 receptor antagonist for the treatment of HIV infection and AID. *Curr Opin. Invest. Drugs* **2007**, *8*, 669−681.

(6) Kwong, P. D.; Wyatt, R.; Robinson, J.; Sweet, R. W.; Sodroski, J.; Hendrickson, W. A. Structure of an HIV gp120 envelope glycoprotein in complex with the CD4 receptor and a neutralizing human antibody. *Nature* **1998**, *393*, 648−659.

(7) Martin, L.; Stricher, F.; Misse, D.; Sironi, F.; Pugniere, M.; Barthe, P.; Prado-Gotor, R.; Freulon, I.; Magne, X.; Roumestand, C.; Menez, A.; Lusso, P.; Veas, F.; Vita, C. Rational design of a CD4 mimic that inhibits HIV-1 entry and exposes cryptic neutralization epitopes. *Nat. Biotechnol.* **2003**, *21*, 71−76.

(8) Zhao, Q.; Ma, L.; Jiang, S.; Lu, H.; Liu, S.; He, Y.; Strick, N.; Neamati, N.; Debnath, A. K. Identification of *N*-phenyl-*N'*-(2,2,6,6-tetramethyl-piperidin-4-yl)-oxalamides as a new class of HIV-1 entry inhibitors that prevent gp120 binding to CD4. *Virology* **2005**, *339*, 213−225.

(9) Madani, N.; Schon, A.; Princiotto, A. M.; Lalonde, J. M.; Courter, J. R.; Soeta, T.; Ng, D.; Wang, L.; Brower, E. T.; Xiang, S. H.; Kwon, Y. D.; Huang, C. C.; Wyatt, R.; Kwong, P. D.; Freire, E.; Smith, A. B., III; Sodroski, J. Small-molecule CD4 mimics interact with a highly conserved pocket on HIV-1 gp120. *Structure* **2008**, *16*, 1689−1701.

(10) Yoshimura, K.; Harada, S.; Shibata, J.; Hatada, M.; Yamada, Y.; Ochiai, C.; Tamamura, H.; Matsushita, S. Enhanced exposure of human immunodeficiency virus type 1 primary isolate neutralization epitopes through binding of CD4 mimetic compounds. *J. Virol.* **2010**, *84*, 7558−7568.

(11) Schon, A.; Madani, N.; Klein, J. C.; Hubicki, A.; Ng, D.; Yang, X.; Smith, A. B., III; Sodroski, J.; Freire, E. Thermodynamics of binding of a low-molecular-weight CD4 mimetic to HIV-1 gp120. *Biochemistry* **2006**, *45*, 10973−10980.

(12) Kwon, Y. D.; Finzi, A.; Wu, X.; Dogo-Isonagie, C.; Lee, L. K.; Moore, L. R.; Schmidt, S. D.; Stuckey, J.; Yang, Y.; Zhou, T.; Zhu, J.; Vicic, D. A.; Debnath, A. K.; Shapiro, L.; Bewley, C. A.; Mascola, J. R.; Sodroski, J. G.; Kwong, P. D. Unliganded HIV-1 gp120 core structures assume the CD4-bound conformation with regulation by quaternary interactions and variable loops. *Proc. Natl. Acad. Sci. U.S.A.* **2012**, *109*, 5663−5668.

(13) Yamada, Y.; Ochiai, C.; Yoshimura, K.; Tanaka, T.; Ohashi, N.; Narumi, T.; Nomura, W.; Harada, S.; Matsushita, S.; Tamamura, H. CD4 mimics targeting the mechanism of HIV entry. *Bioorg. Med. Chem. Lett.* **2010**, *20*, 354−358.

(14) Lalonde, J. M.; Elban, M. A.; Courter, J. R.; Sugawara, A.; Soeta, T.; Madani, N.; Princiotto, A. M.; Kwon, Y. D.; Kwong, P. D.; Schon, A.; Freire, E.; Sodroski, J.; Smith, A. B., III. Design, synthesis and biological evaluation of small molecule inhibitors of CD4-gp120 binding based on virtual screening. *Bioorg. Med. Chem.* **2011**, *19*, 91−101.

(15) Friesner, R. A.; Banks, J. L.; Murphy, R. B.; Halgren, T. A.; Klicic, J. J.; Mainz, D. T.; Repasky, M. P.; Knoll, E. H.; Shelley, M.; Perry, J. K.; Shaw, D. E.; Francis, P.; Shenkin, P. S. Glide: a new approach for rapid, accurate docking and scoring. 1. Method and assessment of docking accuracy. *J. Med. Chem.* **2004**, *47*, 1739−1749.

(16) Halgren, T. A.; Murphy, R. B.; Friesner, R. A.; Beard, H. S.; Frye, L. L.; Pollard, W. T.; Banks, J. L. Glide: a new approach for rapid, accurate docking and scoring. 2. Enrichment factors in database screening. *J. Med. Chem.* **2004**, *47*, 1750−1759.

(17) Fenyö, E. M.; Heath, A.; Dispinseri, S.; Holmes, H.; Lusso, P.; Zolla-Pazner, S.; Donners, H.; Heyndrickx, L.; Alcami, J.; Bongertz, V.; Jassoy, C.; Malnati, M.; Montefiori, D.; Moog, C.; Morris, L.; Osmanov, S.; Polonis, V.; Sattentau, Q.; Schuitemaker, H.; Sutthent, R.; Wrin, T.; Scarlatti, G. International network for comparison of HIV neutralization assays: the NeutNet report. *PLoS One* **2009**, *4*, e4505.

(18) Page, K. A.; Landau, N. R.; Littman, D. R. Construction and use of a human immunodeficiency virus vector for analysis of virus infectivity. *J. Virol.* **1990**, 5270−5276.

(19) Podvinec, M.; Lim, S. P.; Schmidt, T.; Scarsi, M.; Wen, D.; Sonntag, L. S.; Sanschagrin, P.; Shenkin, P. S.; Schwede, T. Novel inhibitors of dengue virus methyltransferase: discovery by in vitro-driven virtual screening on a desktop computer grid. *J. Med. Chem.* **2010**, *53*, 1483−1495.

(20) Kim, Y. A.; Sharon, A.; Chu, C. K.; Rais, R. H.; Al Safarjalani, O. N.; Naguib, F. N. M.; el Kouni, M. H. Synthesis, biological evaluation and molecular modeling studies of N6-benzyladenosine analogues as potential anti-toxoplasma agents. *Biochem. Pharmacol.* **2007**, *73*, 1558−1572.

(21) Siddiquee, K.; Zhang, S.; Guida, W. C.; Blaskovich, M. A.; Greedy, B.; Lawrence, H. R.; Yip, M. L. R.; Jove, R.; McLaughlin, M. M.; Lawrence, N. J.; Sebti, S. M.; Turkson, J. Selective chemical probe inhibitor of Stat3, identified through structure-based virtual screening, induces antitumor activity. *Proc. Natl. Acad. Sci. U.S.A.* **2007**, *104*, 7391−7396.

(22) Tripathy, R.; Ghose, A.; Singh, J.; Bacon, E. R.; Angeles, T. S.; Yang, S. X.; Albom, M. S.; Aimone, L. D.; Herman, J. L.; Mallamo, J. P. 1,2,3-Thiadiazole substituted pyrazolones as potent KDR/VEGFR-2 kinase inhibitors. *Bioorg. Med. Chem. Lett.* **2007**, *17*, 1793−1798.

(23) Lyne, P. D.; Lamb, M. L.; Saeh, J. C. Accurate prediction of the relative potencies of members of a series of kinase inhibitors using molecular docking and MM-GBSA scoring. *J. Med. Chem.* **2006**, *49*, 4805−4808.

(24) Bembenek, S. D.; Keith, J. M.; Letavic, M. A.; Apodaca, R.; Barbier, A. J.; Dvorak, L.; Aluisio, L.; Miller, K. L.; Lovenberg, T. W.; Carruthers, N. I. Lead identification of acetylcholinesterase inhibitors-histamine H3 receptor antagonists from molecular modeling. *Bioorg. Med. Chem.* **2008**, *16*, 2968−2973.

(25) Ravindranathan, K. P.; Mandiyan, V.; Ekkati, A. R.; Bae, J. H.; Schlessinger, J.; Jorgensen, W. L. Discovery of novel fibroblast growth factor receptor 1 kinase inhibitors by structure-based virtual screening. *J. Med. Chem.* **2010**, *53*, 1662−1672.

(26) Zhang, H.; Bhattacharya, S.; Tong, X.; Waheed, A. A.; Hong, A.; Heck, S.; Curreli, F.; Goger, M.; Cowburn, D.; Freed, E. O.; Debnath, A. K. A cell-penetrating helical peptide as a potential HIV-1 inhibitor. *J. Mol. Biol.* **2008**, *378*, 565−580.

(27) Jiang, S.; Lu, H.; Liu, S.; Zhao, Q.; He, Y.; Debnath, A. K. N-Substituted pyrrole derivatives as novel human immunodeficiency virus type 1 entry inhibitors that interfere with the gp41 six-helix bundle formation and block virus fusion. *Antimicrob. Agents Chemother.* **2004**, *48*, 4349−4359.